Samarendra Basu,[1] *Ph.D.*

Formation of Gunshot Residues

REFERENCE: Basu, S., **"Formation of Gunshot Residues,"** *Journal of Forensic Sciences,* JFSCA, Vol. 27, No. 1, Jan. 1982, pp. 72-91.

ABSTRACT: Scanning electron microscopy combined with energy dispersive X-ray analysis (SEM-EDX) was used to determine new structural criteria to further substantiate the view that gunshot residue (GSR) particles have a characteristic structure. Because GSR particles are formed by rapid cooling from extreme temperatures and high pressures, they should contain features of condensates not only on their surfaces, but also within their interiors. Both the surfaces and the cross sections of GSR were examined for X-ray mapping of elements and for topographic analysis. Vaporized lead, antimony, and barium may condense uniformly and concurrently, or irregularly and discontinuously, or as a layer of lead around a nucleus of barium and antimony. These three modes of GSR formation may correspond to the equilibrium state, the increasing temperature state, and the decreasing temperature state of the explosion gas mixture of the priming compound. Most GSR smaller than 10 μm are formed as droplets at equilibrium. Larger spheres grow by coalescence of the smaller droplets. These residues pass through various metastable forms and then freeze. Only a few semisolid spheroids of barium and antimony may capture lead vapors of the etched bullet and burnt residues, and these appear as "peeled oranges."

KEYWORDS: criminalistics, gunshot residue, chemical analysis, SEM-EDX, particle sectioning, X-ray mapping analysis

The current view of gunshot residue (GSR) using scanning electron microscopy with energy dispersive X-ray analysis (SEM-EDX) is that GSR particles possess a characteristic spheroidal shape, a unique composition caused by primer-derived and bullet-derived elements (mainly lead, antimony, and barium), and a diameter which is most often in the range of 0.1 to 10 μm and, occasionally, up to 55 μm or above [*1-6*]. In fact, this particle morphology, when combined with the elemental composition, makes GSR quite distinct from many environmental particulates, including occupational particles such as lead aerosols, automobile exhaust, and condensation fumes that may contain one or more elements of GSR [*7,8*]. Knowing the origin and the formation GSR is essential to knowing the difference between them and the environmental particles. Unlike many solid vapors that grow as prisms, dendrites, and other forms of crystals [*7,9,10*], GSR particles form as droplets before they solidify. This process and the rigid conditions involved, such as steep rises in temperature and pressure and their equilibria [*11*], make GSR unique products of primer explosion.

This report establishes that GSR particles are condensates not only in their surface morphology, which three earlier reports [*2,6,12*] suggest, but also in their interiors in terms of distribution of lead, antimony, and barium. Both the surfaces and the cross sections of GSR

Received for publication 30 March 1981; revised manuscript received 11 May 1981; accepted for publication 13 May 1981.

[1]Research scientist III, New York State Police Crime Laboratory, Building 22, State Campus, Albany, NY 12226.

have been studied for X-ray mapping of elements and for topography with the SEM-EDX technique. Incidentally, the method introduced for sectioning of GSR is applicable to other microscopic particles. Matricardi and Kilty [*3*] were the first to study element distribution in the interior of GSR by fracturing them with a scalpel, but their studies were limited to only a few large primer cup particles (diameter, 120 μm). The present results strongly corroborate the current view that GSR particles do, in fact, possess a characteristic structure.

Materials and Methods

GSR Collection from the Firing Hand

GSR particles were collected from the firing hand by a modified "glue-lift" technique [*6*]. The modification was to improvise inexpensive collectors made of plastic thimbles (Caplugs®). In each collector, one thimble was used to mount the usual collection disk [*6*], namely, a polished carbon planchet (diameter, 13 mm [1/2 in.]; thickness, 3 mm [1/8 in.]), while another thimble covered the planchet from the top. The planchet contained a spread, thin layer (thickness 2 μm) of rubber cement used as diluted (five times) with 1,1,1-trichloroethane. With a finger inserted into a thimble, the attached planchet was gently touched five times to a specific area: either the palm or the back of a particular hand, as marked on the side of each thimble. Thus, two collections were made from each hand with the total collections being four per suicide victim or per test firing. In routine test firing both hands of the shooter were thoroughly cleaned prior to shooting [*6*].

Mounting, Embedding, and Sectioning

The GSR particles were collected for sectioning in two ways. In the first method the particles emanating from a fired gun (three to five firings) were trapped on aluminum targets, made sticky to capture the residues. Aluminum foil (Reynolds Wrap) was cut into six to ten pieces, each 13 mm (1/2 in.) wide and 102 mm (4 in.) long. The sticky medium applied to the foil was Epoxy-812, which was also the GSR embedding medium. As per instructions received from the suppliers (Ernest F. Fullam, Inc.), the epoxy was mixed with two anhydrides (nadic methyl anhydride and dodecenyl succinic anhydride) and then applied to the aluminum targets fixed in place on two cardboards. One piece of cardboard was held alongside the trigger 50 mm (2 in.) from the trigger. Another piece of cardboard was held horizontally about 100 mm (4 in.) below the exit of the muzzle.

In the second method large quantities of GSR were collected by shaking them off primer cups of expended bullet casings—about 50 casings each time. These particles were then sieved through a 300-μm hole in a cup-shaped electron gun aperture for Advanced Metals Research Corp. Model AMR-1000 microscope and spread on the adhesive layer of a piece of Scotch® copper tape 8 by 100 mm (1/3 by 4 in.). Aluminum foil can also be used. Both aluminum and copper are flexible and soft enough for sectioning.

For the sake of convenience, we will call those particles captured on aluminum targets "target GSR" and those collected from primer cups "primer GSR." The rest of the procedure was the same for either kind of GSR and is described in Fig. 1. The accelerating compound (DMP-30) was added to the epoxy mixture just prior to the final application of the mixture on the aluminum foil or the copper tape (Fig. 1a and b). The beam capsule (plastic; diameter, 9.5 mm [3/8 in.]; length, 19.05 mm [6/8 in.]) containing the spool of foil and the epoxy mixture was stored at 65°C for 6 h and, then, for another five days at room temperature. Epoxy hardened during this period. The capsules were sectioned in a microtome (Will Corp.) with the blade (steel) being inclined to the axis of the capsule at a 75° angle. Because the embedment was usually brittle, it was advantageous to cut sections of whole capsules. The section thickness was in the range of 40 to 200 μm. Thick sections were preferred for primer GSR because of their larger size and brittleness.

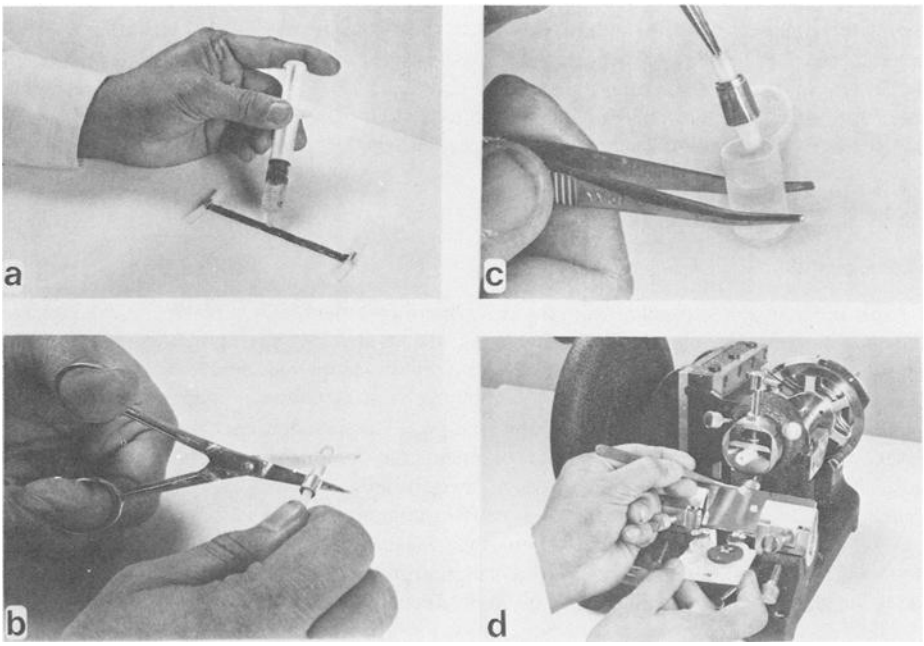

FIG. 1—*Combined mounting, embedding, and sectioning of GSR.* (a) *Epoxy-812 mixed with its hardener and accelerator is taken in a syringe and applied to GSR previously spread on the adhesive side of Scotch copper tape. The copper tape is held at two ends by soft plastic tubing.* (b) *The copper tape is rolled over one piece of tubing while the other piece of tubing is kept fixed. The rolled tubing is cut on both sides of the copper spool.* (c) *The copper spool is inserted into a beam capsule filled with the epoxy mixture. The capsule is covered and epoxy is allowed to harden.* (d) *The sections are made in a microtome with a steel blade.*

Microscopy of GSR and Their Cross Sections

The procedure used to search for GSR in the scanning electron microscope has been described elsewhere [*6*]. The carbon planchets containing GSR were lifted off the thimble collectors before being examined. The sections of GSR were also mounted on carbon planchets. All specimens were studied at 20 kV in a SEM (AMR 1000) in conjunction with an energy dispersive X-ray analyzer (EDAX-707A). Although the planchets containing GSR were usually coated with evaporated carbon (20 nm) to avoid charging effects, this coating was not applied to cross sections of GSR until X-ray analysis (mapping) of all elements (lead, antimony, and barium) was complete. Owing to the presence of aluminum or copper foil in the background, the charge buildup was not serious enough to affect backscattered electrons and X-rays.

The cross sections were distinguished from partial sections by the presence of lead, antimony, and barium. The search of GSR cross sections was also facilitated by the fact that the sections occurred only in between successive turns of the foil. The backscattered electron mode was particularly useful in the search process. This is due to atomic number contrast [*13*] and higher backscattering [*14*] by the heavier elements (lead, barium, and antimony) of GSR (compare with data from Ref *15*). Also, the brightness and shadows in the backscattered electron image of a GSR cross section clearly showed whether the emitted X-rays were reaching the X-ray detector or whether they were being obstructed by irregularities in the cross section. This verification was made possible in the AMR 1000 because the two detectors for backscattered electrons and for X-rays are close. The secondary electrons cannot show these obstructions because they do not travel in straight lines [*14*]. As mentioned under

"Results," gold coating was applied to some GSR and to some GSR cross sections to enhance the topographic contrast with the secondary electrons.

X-Ray Mapping of Elements

To obtain an acceptable X-ray map in the SEM-EDX, it was desirable to collect a total of 50 000 to 400 000 counts in the integrated micrograph [*16*]. This was achieved by the following steps:

(a) using a larger aperture of the final lens, for example, 200 μm instead of 100 μm, which one normally uses for imaging in the SEM;

(b) increasing the incident beam current, that is, using the spot size at 3 in the AMR 1000;

(c) adjusting the tilt angle of the specimen to about 45°, which effectively increases the X-ray take-off angle and collection (compare with Fig. 16 in Ref *17*);

(d) working at an optimal working distance (6 to 8 mm), which also enhances the take-off angle and reduces the distance between the specimen and the X-ray detector (silicon wafer); and

(e) mapping the specimen at a slow scan rate, which was essential to avoid pulse pileup during dead time of the analyzer [*18*].

The maximal integral (pileup) count with the EDAX memory is 263 744 (compare with 2^{18} for 18 bits). This number was used to estimate the length of scanning time in the recording mode. As specified in the figure captions of some GSR cross sections, the tilt angle had to be adjusted occasionally from about 0 to 18°. Otherwise, the tilt was at a 45° angle in line with the detector (X-ray) axis for most specimens. With a given element a window was set at the strongest peak of the element (for example, Lα lines of antimony and barium and M line of lead), and the window width was adjusted to two thirds of half-hand width of the peak. Usually this width corresponded to two to six channels, each channel being 50 eV in the 0-20-keV scale. The adjustments in Steps (a) to (e) were made until the readout of the multichannel analyzer showed a count rate of 100 to 500 cps. Depending on the count rate and the peak intensity, the total picture time was varied from 4 to 12 min. Repeated exposures were made to achieve sharper maps. The net exposure time (4 to 8 min) was not the same for antimony and barium. With lead the exposure time was much increased (12 min) to share X-rays from both M and L peaks (Lα) so that the combined emission (M and L) reached the X-ray detector from both low and high take-off angle areas of the specimen.

Results

Elements Studied

The main emphasis of this report is on the formation of primer-derived GSR, each of which contains the elements of the priming compound, mainly lead, antimony, and barium. Reference will be given only to those three elements in this section. The elements of lead, copper, and iron and other nonspecific elements, such as aluminum, silicon, sulfur, potassium, and calcium, are often found in some GSR, originating from various sources that include the etched bullet and its casing. The formation of these bullet-derived GSR and the bullet particles has been well documented in a recent report by Wolten and Nesbitt [*12*].

Condensate Morphology

Gunshot residues are generally spheroids, but owing to their characteristic surface features, a majority of them fall into three distinct morphologic categories. These are regular spheroids (Fig. 2a, b, c, and d), nodular spheroids (Fig. 2f, g, h, and i), and irregular spheroids (Fig. 3a, b, and c). Selected GSR for each category have been arranged in a sequence whereby one can recognize the condensate appearance of GSR by studying the formative

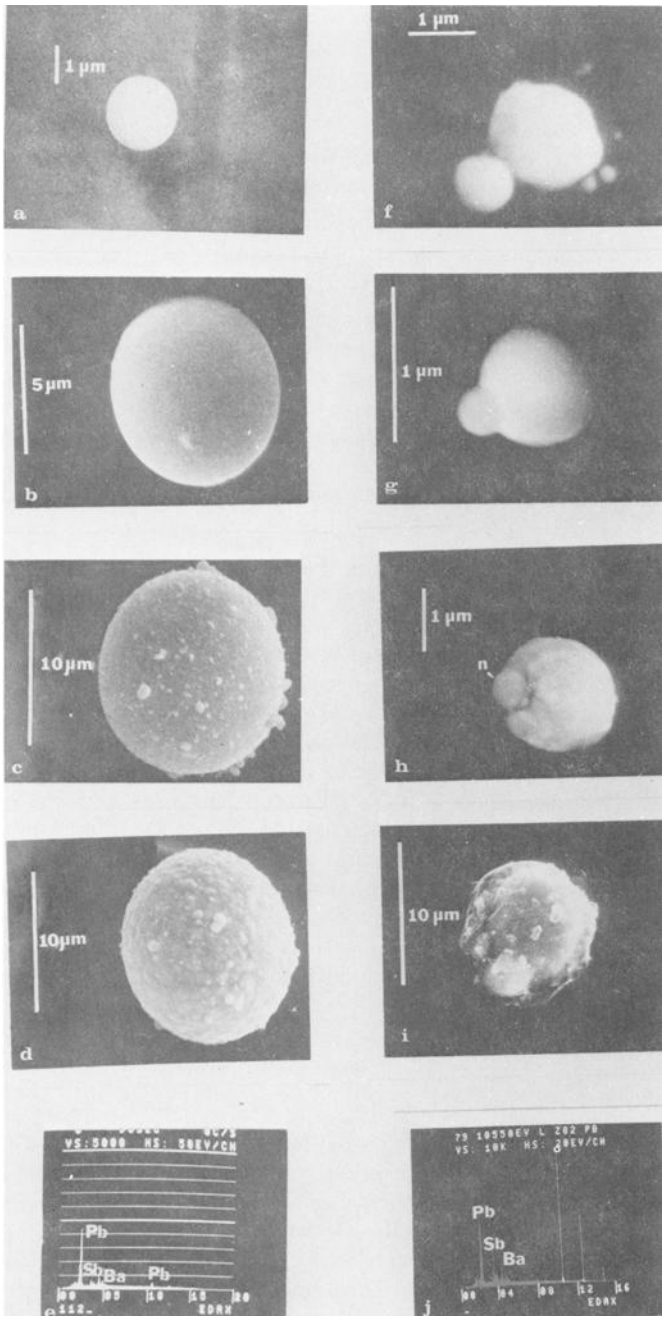

FIG. 2—*GSR spheroids, regular and nodular, obtained by glue-lift* [6]. *The variation in their morphologies is suggestive of their formation.* (a, b, c, *and* d) *Regular spheroids and* (e) *their representative X-ray emission spectrum.* (f, g, h, *and* i) *Nodular spheroids and* (j) *their representative X-ray emission spectrum;* (n) *indicates nodule* (h). *Sources of GSR:* (a *and* h) *a suicide victim's right hand; .22 caliber revolver (Harrington & Richardson) .22 long rim-fire federal cartridge;* (b *to* d, g, *and* i) *one test firing with a .38 caliber Smith & Wesson revolver using Remington .38 Special 200 grain lead bullets; and* (f) *one test firing with a pump action 12-gauge shotgun (Winchester Model 1200) using 70-mm (2¾ in.) 00 buckshot.*

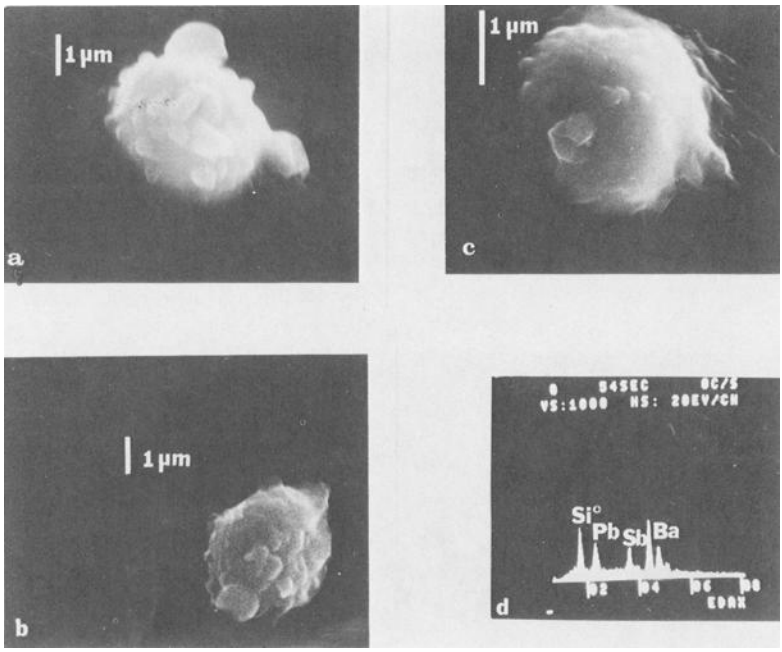

FIG. 3—*Irregular GSR spheroids* (a-c) *possessing unstable features and their representative X-ray emission spectrum* (d), *obtained by glue-lift* [6]. *The three GSR particles originated from three individual firings with a .38 caliber Smith & Wesson revolver. Ammunition was the same as in Fig. 2b-d, g, and i.*

stages implicit in the GSR morphologies. Yet these GSR particles have the same elements, namely, lead, antimony, and barium, as shown by the representative X-ray emission spectrum at the bottom of each figure (see Fig. 2e and j). Furthermore, these GSR particles originated from different guns and ammunition. The surface of the regular spheroids varies from a smooth to a knobby appearance (Fig. 2a, b, c, and d). The nodular spheroids are apparently the products of fusion between a small spheroid and a larger spheroid (Fig. 2f, g, h, and i). The irregular spheroids have larger knobs and spikes and a general shape showing great instability (Fig. 3a, b, and c), perhaps resulting from extreme thermal conditions. The liquid drop model of condensation [*19,20*] suggests that regular spheroids are the most stable among these configurations of a condensate droplet. According to this model, GSR larger than those shown in Figs. 1, 2, and 3 may be observed because they will grow by coalescence of the smaller spheres. In fact, GSR up to 55 μm in diameter, such as those that look like peeled oranges (Fig. 4a, c, and e), and "hollow-shaped" GSR (Fig. 5) are occasionally obtained from the firing hand by glue-lift collection [*6*]. The "peeled oranges" have a distinct core and an outer leaflet (Fig. 4e). Each hollow-shaped GSR has a large cavity and several small holes (Fig. 5).

It was important to know whether the distribution of elements inside the GSR cavities and cores differs from that on the GSR surface. In a preliminary attempt, the author used a focused electron beam, which others [*3*] have also used. The loss of X-rays because of low take-off angles was minimized by keeping the specimen in line with the axis of the X-ray detector and then rotating the GSR, and by varying the tilt angle (Fig. 5a, b, and c) until the particle feature was sufficiently oblique to the incident electrons to give the highest collection of X-rays. The partial field (AMR 1000) was used to avoid going to much higher magnifications where the beam current and the X-ray counts per second diminish sharply. When the electron spot was made incident to the cavity (marked *e* in Fig. 5) of the hollow-shaped GSR,

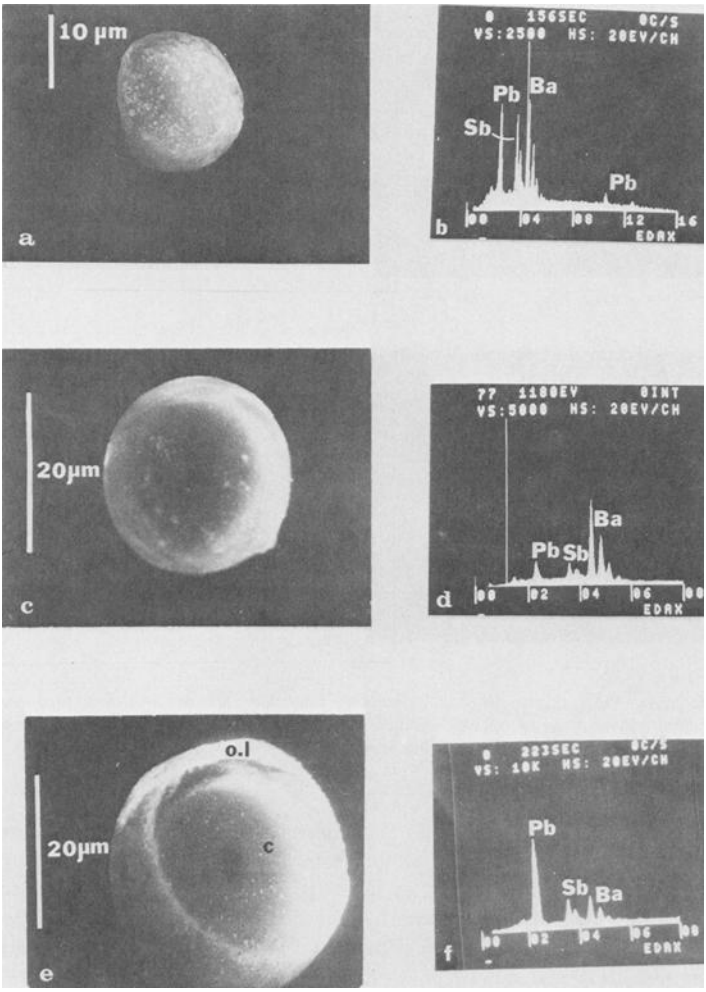

FIG. 4—*Three "peeled oranges" (GSR)* (a, c, *and* e) *and their respective X-ray emission spectra* (b, d, *and* f) *by glue-lift* [6]. *Notations:* c, *core and* o.l, *outer leaflet of a "peeled orange." Sources of GSR:* (a *and* b) *a suicide victim's right hand (same as in Fig. 2a and h);*(c *and* d) *one test firing with a 9-mm caliber Walther PPK/S pistol using .380 automatic 95-grain Western ammunition;* (e *and* f) *one test firing with a .38 caliber Smith & Wesson revolver (same as in Fig. 2b–d, g, and i).*

the peak due to only barium appeared in the X-ray spectrum (*e* in Fig. 5). As the electron spot was brought onto the top surface of the same GSR (marked *f* in Fig. 5), the peaks due to antimony and lead appeared (Fig. 5f). A similar result had been observed earlier with the "peeled oranges" and was reported elsewhere [*6*]. The core of "peeled oranges" showed only the barium peaks. Antimony and then lead peaks were detected as the electron spot was moved toward the periphery of the GSR, lead being the outermost. When the entire particle was on the screen, the composite spectrum showed the three elements lead, antimony, and barium (Fig. 4b, d, and f for three "peeled oranges"; Fig. 5d for a hollow-shaped GSR).

X-Ray Mapping of Surface Elements

The previous method does not correct for the varying absorption of X-rays into the specimen with take-off angle and the matrix interelement effect. X-ray emission from an irregular

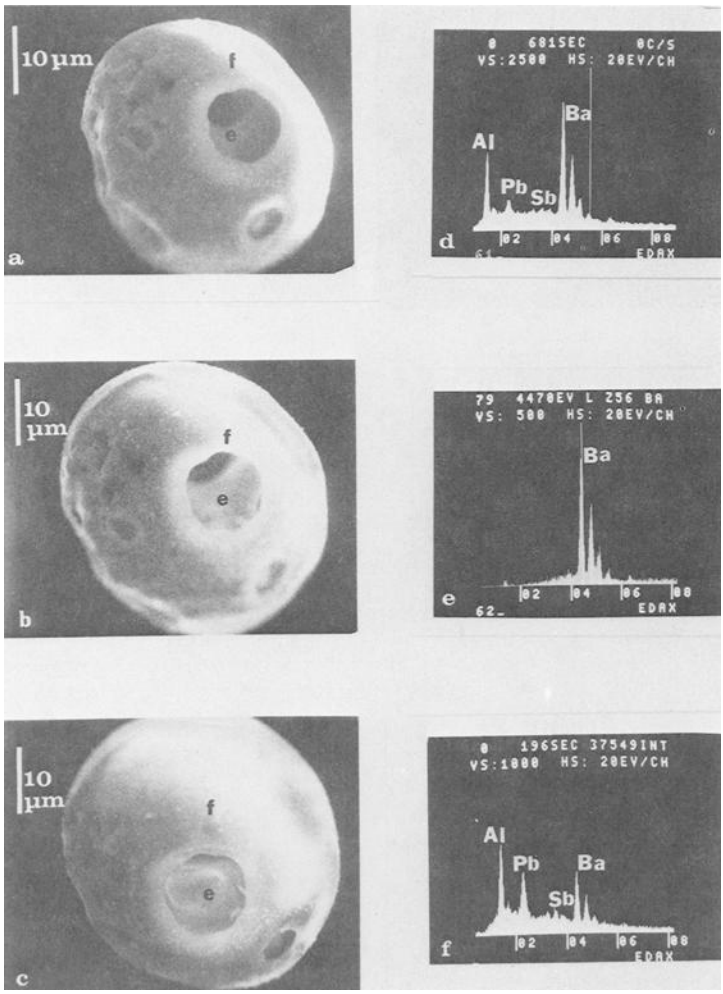

FIG. 5—*A hollow-shaped particle obtained by glue-lift* [6] *from one firing with a semiautomatic Remington Model 1100 shotgun. The GSR was examined at three tilts in line with the axis of the X-ray detector. Tilts* (a) *45°,* (b) *+16°, and* (c) *−16°. Sources of X-ray emission spectra:* (d) *whole particle,* (e) *the large cavity marked* e, *and* (f) *surface of the GSR.*

surface can be misleading because of these two effects [*16*]. More particularly, because the penetration depth of 20 kV electrons is very limited with higher atomic number elements, the sampling volume [*21*] in which the X-rays of interest are generated is relatively less compared to the size of large GSR. The low energy X-ray emissions, such as the M lines of lead and the L lines of antimony, which are created deep inside large GSR (diameter, >7 µm), are easily absorbed before they can leave the particle surface. The effect causes a partial particle view in the X-ray maps of the corresponding elements (Fig. 6). The effect is not observed with GSR of diameter below 7 µm.

The GSR in Fig. 6a has several features: a peeled orange, a hole marked *h*, and a nodule marked *n*. The composite X-ray spectrum of the particle is shown in Fig. 6f. It has been determined that direct negatives give better contrast of the dotted X-ray maps (Fig. 6b for lead, 6c for antimony, 6d for barium, and 6e for lead plus aluminum plus silicon) than positive prints from them, and this convention has been followed throughout this report. Barium is the only element that gives a large yield of X-rays from the entire particle to the in-line detec-

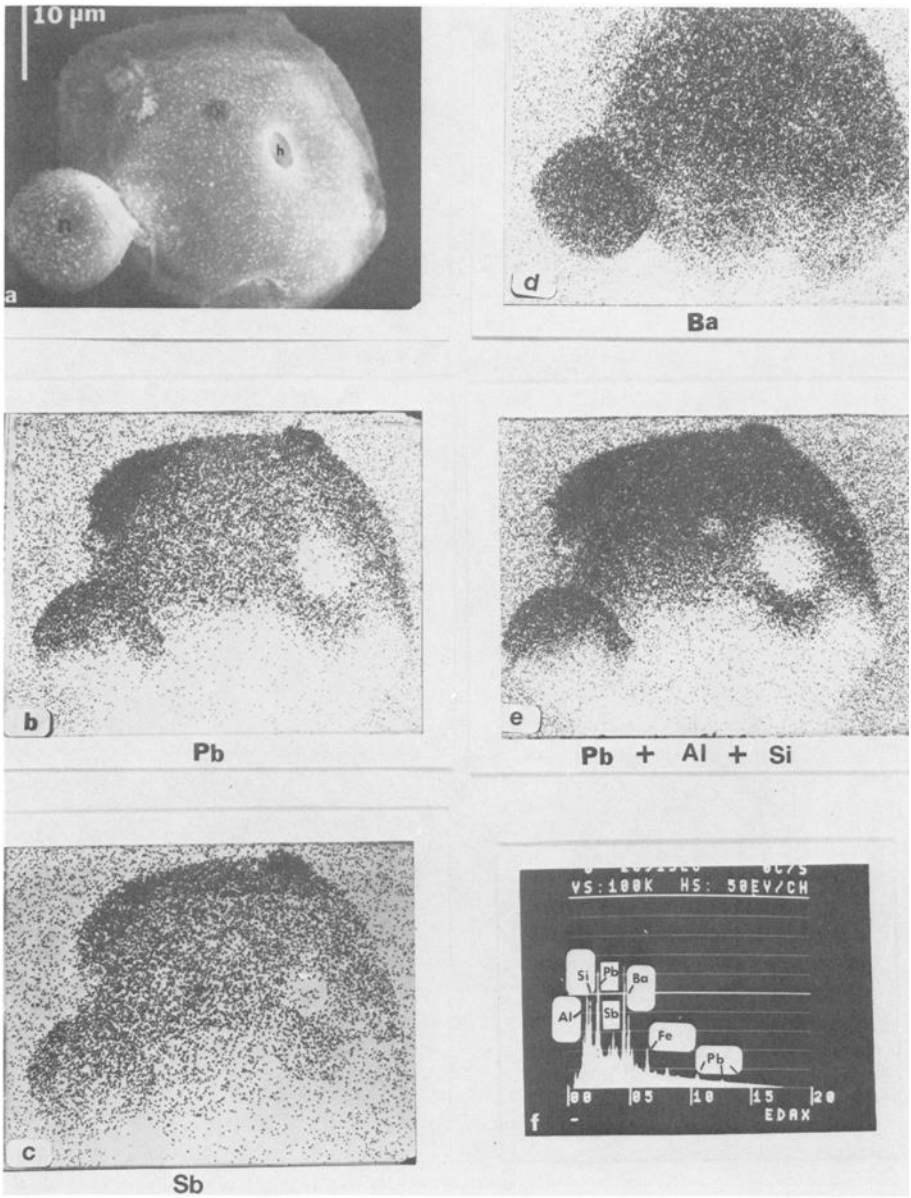

FIG. 6—*Morphology of an atypical GSR and X-ray maps of lead, antimony, and barium on this GSR surface. Notations:* n, *nodule and* h, *hole.* (a) *Morphology,* (b) *lead map,* (c) *antimony map,* (d) *barium map,* (e) *lead, aluminum, and silicon maps (superimposed), and* (f) *composite X-ray emission spectrum of the GSR. The GSR was obtained by glue-lift* [6] *following one firing with a hinge frame 12-gauge shotgun manufactured in Brazil. Ammunition was 70-mm (2¾-in.) 00 buckshot.*

tor (Fig. 6d). The other maps (Fig. 6b, c, and e) show that lead and antimony emissions (M and Lα lines) and the emissions from the aluminum and silicon (K lines) rarely reach the detector from the bottom half of the GSR. (The lead map [Fig. 6b] included both the Lα and M emissions of lead [see Materials and Methods.]) These results suggest that for semiquantitative analysis of element distribution in GSR, one needs a method that will provide cross sections of GSR.

Collection for Sectioning

Let us refer to the method in Fig. 1 that enables one to make sections of GSR. Target GSR are up to 55 μm in diameter (see Figs. 2 to 5). Primer GSR are much larger and, therefore, are easily checked in a light microscope, as shown in Fig. 7a and b. They are generally spheroids with a diameter up to 270 μm on occasion (see arrowhead in Fig. 7c). When these spheroids are examined in the SEM-EDX, they exhibit the X-ray emissions of lead, antimony, barium, and occasionally silicon (Fig. 7d).

Mounting and Sectioning

Figure 8a is a low magnification view in the SEM of a cut section through a beam capsule, which contains the embedment of target GSR from an experiment consisting of three test firings. Since the aluminum foil target is rotated onto a spool, GSR sections are found in concentric circles between successive turns of the foil (Fig. 8b, arrow). It is suggested that this new technique of particulate sectioning be called "combined mounting and embedding in circles." This technique is a significant advance over embedding and sectioning in suspension, such as in cytology, for an important reason. Because the GSR are held in place in epoxy, they are easily localized between successive turns of the foil. This reduces the search time, especially in the backscattered electron mode (Fig. 8b). Wherever topography is needed, the image mode is changed to secondary electrons (Fig. 8a).

The limitation of the present technique is determined by the lack of closeness between successive turns of the foil because the foil-spool eventually swells in the embedding medium inside

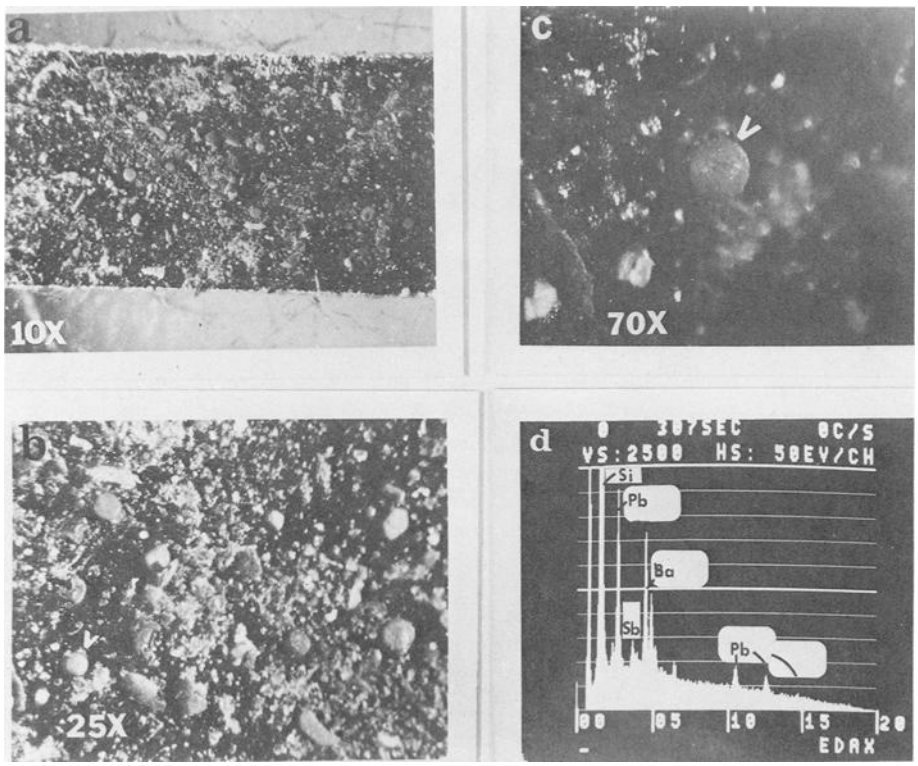

FIG. 7—*Primer GSR particles on the adhesive side of a Scotch copper tape.* (a, b, *and* c) *Light microscopic views. Arrowhead indicates a GSR spheroid of diameter 270 μm* (c). (d) *X-ray emmission spectrum of the GSR shown by the arrowhead in* (c).

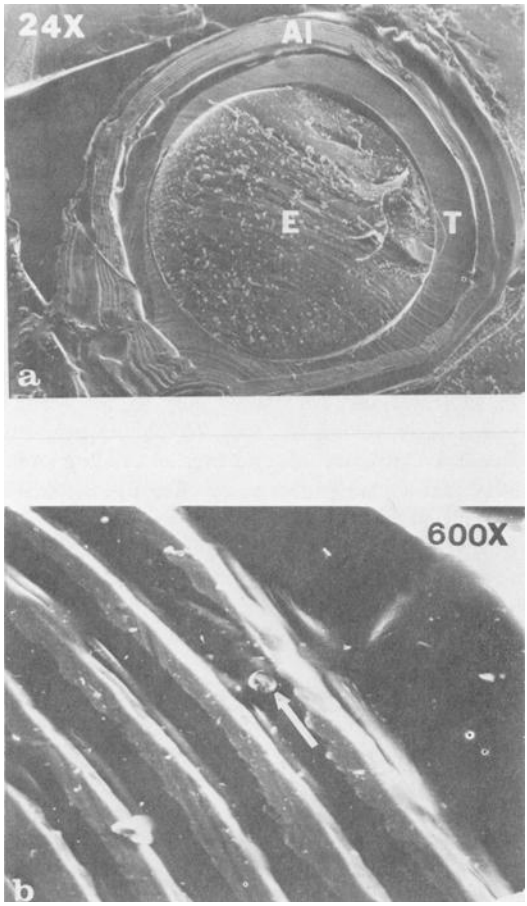

FIG. 8—*SEM images of a sectioned beam capsule containing target GSR in a spool of aluminum foil.* (a) *Secondary electron image.* (b) *Backscattered electron image. A sectioned GSR is shown by an arrow. Notations:* Al, *turns of aluminum foil;* E, *Epoxy-812 (embedding medium); and* T, *plastic tubing containing the rolled aluminum foil.*

the beam capsule. Therefore, particles below 2 μm in diameter are seldom sectioned. This situation might be improved by keeping the spool in a much tighter configuration. For example, one could use a beam capsule of a diameter comparable to that of the spool diameter and apply the method with a better embedding medium so that small particles would seldom be pushed aside while being sectioned. Epoxy-812 was the resin selected from among the many embedding media that have been tried. None of the wet methods using organic solvents, such as chloroform and petroleum ether, work well for collecting and concentrating the GSR from glue-lift disks because the GSR elements variably dissociate in those liquids, as well as in water.

Topography of Sectioned GSR

Figure 9a, b, and c shows three typical cross sections of primer GSR in the diameter range of 70 to 80 μm. The larger the GSR, the greater the chance of features like sponginess, hollows, and cavities in these cross sections. The cavity of the cross section in Fig. 9c is a distinct evidence of an air pocket.

FIG. 9—*Surface topography (secondary electron image) in the SEM of three cross sections of primer GSR (diameter, 70 to 80 μm). Notation:* c, *large cavity in* (c). *The cross sections in* (a *and* b) *were gold and carbon coated.*

X-Ray Mapping of Elements in Cross Sections

A total of 227 cross sections of target and primer GSR were studied in detail as they appeared on the screen. A criterion for their selection was that each cross section have all the principal elements, lead, antimony, and barium. The distribution of these elements in these cross sections falls into three distinct categories (I to III), summarized in Table 1.

Figures 10 to 12 show the surfaces, the X-ray maps, and the composite X-ray spectra of lead, antimony, and barium in typical GSR cross sections. Two cross sections are shown for each category (I to III) of element distribution. The panel arrangement in Figs. 10 to 12 is

TABLE 1—*Distribution of lead, antimony, and barium in GSR cross sections.*[a]

Type of Element Distribution	Number of GSR Cross Sections	Range of Cross-Section Diameters, μm	% in each GSR Group (T or P)
Category I: uniform and concurrent (lead, antimony, barium)	80 (T)	2-10	68
	65 (P)	8-30	59
Category II: inhomogeneous and discontinuous distribution or both (lead, antimony, barium)	30 (T)	15-55	25
	39 (P)	22-130	35
Category III: distribution in layers (lead around a barium and antimony core)	6 (T)	10-35	5
	7 (P)	16-74	6

[a]Total number of target GSR cross sections, obtained from 182 slices of embedded capsules, was 116. Total number of primer GSR cross sections, obtained from 19 slices of embedded capsules, was 111. The success rate in obtaining cross sections was ninefold more with the primer GSR than with the target GSR. T = target GSR; P = primer GSR.

such that the lower panels (f to j) indicate a minor deviation from the trend in the results in the upper panels (a to e).

The smaller target GSR of cross-sectional diameter 2 to 10 μm belong in Category I, as shown in Fig. 10. The cross section in Fig. 10a was shown earlier in Fig. 8b at a much lower magnification. The cross-sectional diameter is up to 30 μm for the primer GSR of the same category (Table 1). The observed optical densities in individual X-ray maps of elements in Fig. 10 (b to d) and (g to i) suggest that the distribution of lead, antimony, and barium is homogeneous. This means that these elements condensed uniformly and concurrently. This distribution represents 59 to 68% of all GSR cross sections studied. Additionally, the lower panel (g to i) of Fig. 10 shows that lead is more prominent than antimony and barium toward the edge of the GSR cross section (Fig. 10f). This cross section (Fig. 10f) is also smoother than the one in Fig. 10a. Notice the sharper contour of this cross section in the lead map (Fig. 10g). This was parallel to the emergence of the higher energy emissions (L lines) of lead in the composite X-ray spectrum (compare Figs. 10j and 10e). The strong silicon peak (K line) is from the cross sections (Fig. 10) of GSR. The X-ray maps show that silicon is also homogeneous, the same as lead, antimony, and barium. The significance of silicon is not clear, and maps having this element have been omitted. Silicon may be nonspecific as it is often absent from some GSR particles.

In Category II, as shown in Fig. 11 (a to e), the distribution of elements in the GSR cross section is irregular and discontinuous. The lower panel (Fig. 11 f to j) shows that the bulk of the cross section contained a rather homogeneous distribution of elements, but heterogeneity occurred in it because of a final irregular mass distribution. Since the larger GSR of diameters above 22 μm mainly belong to this category, the discontinuous deposits of lead, antimony, and barium reflect a time-dependent process—perhaps the growth of these GSR or other events that created the holes and air pockets (cavities) in the interior of these particles. The GSR cross sections in Category II constitute about 25 to 35% of the total GSR cross sections studied (Table 1).

In Category III, which was the minority (5 to 6% of total) group, lead occurs as a ring-like layer (width, 3 to 4 μm) around a core at the center (Fig. 12, upper panel). The core usually contains a uniform distribution of antimony and barium. The bulk of the cross section in the upper panel (a to e) of Fig. 12 is due to the core. In the lower panel (f to j), however, the lead ring is much wider and the core (antimony and barium) is eccentric. An eccentric core may be the indication of air drag resulting from a higher velocity of the GSR. Interestingly, the cross section in the lower panel was a target GSR, whereas the cross section in the upper panel was of a primer GSR. The cross sections of target GSR in this category were usually 10 to 35 μm (Fig. 12, a to e). Much larger cross sections (for example, 55 μm in Fig. 12 f to j)

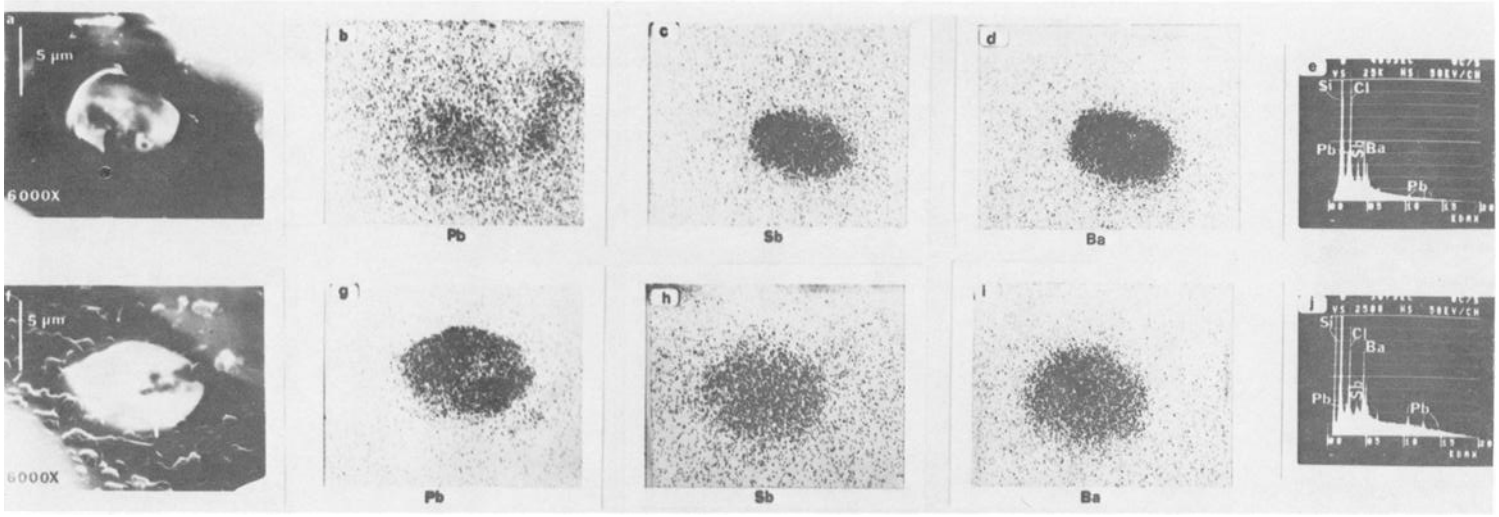

FIG. 10—*Lead, antimony, and barium distribution of Type I (homogeneous) in cross sections of two target GSR (trigger residues) (diameters, 6 to 8 μm). Upper panel:* (a) *SEM image (backscattered) at 45° tilt angles,* (b) *lead map,* (c) *antimony map,* (d) *barium map, and* (e) *composite X-ray emission spectrum of the field containing the cross section in* (a). *Lower panel:* (f) *SEM image (backscattered) at 45° tilt angle,* (g) *lead (Pb) map,* (h) *antimony (Sb) map,* (i) *barium (Ba) map, and* (j) *composite X-ray emission spectrum of the field containing the cross section in* (f). *The chlorine peak in* (e) *and* (j) *is due to background epoxy.*

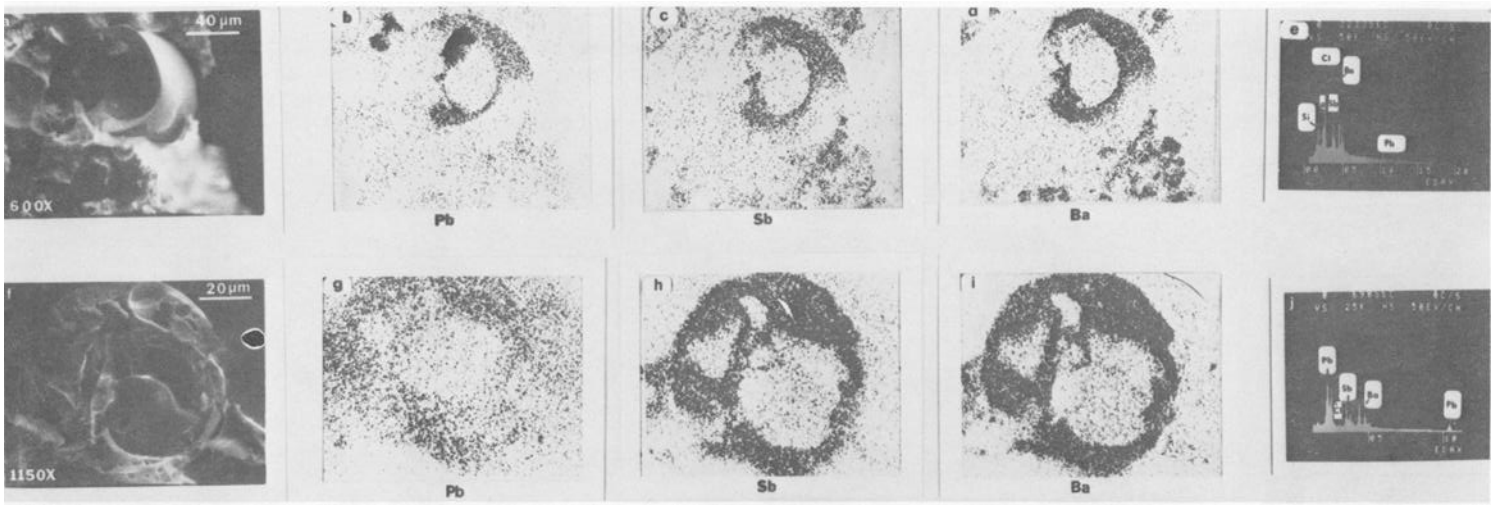

FIG. 11—*Lead, antimony, and barium distribution of Type II (heterogeneous) in cross sections of two primer GSR (primer cup particles) (diameters, 70 to 80 μm). Upper panel:* (a) *SEM image (secondary) at 0° tilt,* (b) *lead map,* (c) *antimony map,* (d) *barium map, and* (e) *composite X-ray emission spectrum of the field containing the cross section in* (a). *Lower panel:* (f) *SEM image (secondary) at 18° tilt angle,* (g) *lead (Pb) map,* (h) *antimony (Sb) map,* (i) *barium (Ba) map, and* (j) *composite X-ray emission spectrum of the field containing the cross section in* (f). *Chlorine peak in* (e) *and* (j) *is due to background epoxy.*

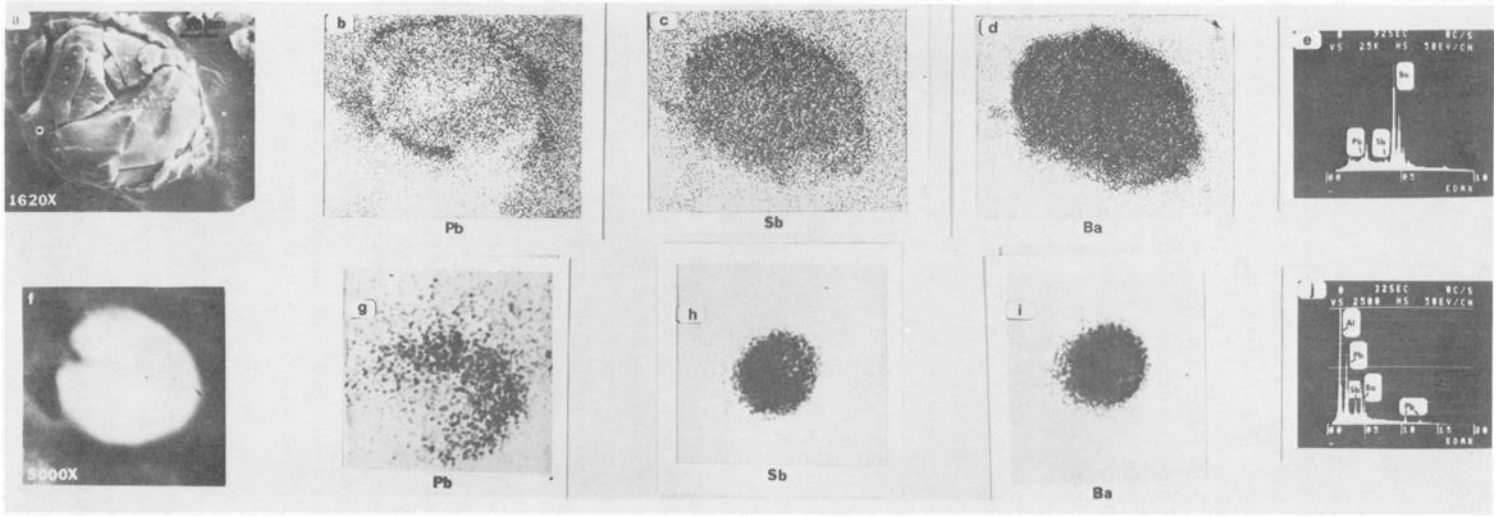

FIG. 12—*Lead, antimony, and barium distribution of Type III, that is, lead as a layer around a barium-antimony core, in cross sections of a primer GSR and a target GSR. Upper panel:* (a) *SEM image (secondary) at 45° tilt angle of a primer GSR cross section (diameter, 55 μm). The cross section was coated with gold and carbon after all X-ray maps were obtained,* (b) *lead map,* (c) *antimony map,* (d) *barium map, and* (e) *composite X-ray emission spectrum of the field containing the cross section in* (a). *Lower panel:* (f) *SEM image (backscattered) of a target GSR (muzzle residue) cross section (diameter, 10 μm) at 0° tilt angle,* (g) *lead map,* (h) *antimony map,* (i) *barium map, and* (j) *composite X-ray emission spectrum of the field containing the cross section in* (f). *The aluminum peak in* (j) *is due to the aluminum foil in the background. The chlorine peak due to background epoxy is not marked.*

were found with primer GSR (Table 1). The distribution of lead, antimony, and barium in layers in Category III supports the earlier observation of Matricardi and Kilty [*3*] concerning some fractured primer cup particles.

Analysis

The distribution of elements in the previous categories (I to III) has certain features that correlate with the GSR morphologies (Figs. 2 to 5), such as the lead ring and the outer leaflet of "peeled oranges." Also, the size range is a common denominator. This correlative analysis suggests that most regular spheroids (Fig. 2a to d), nodular spheroids (Fig. 2f to i), and irregular spheroids (Fig. 3) in the size range of 2 to 10 μm fall into Category I; that is, they have a homogeneous distribution of elements in their interior. Dense spots from lead and other nonspecific elements (aluminum, potassium, sulfur, calcium, iron, and copper) except silicon are rarely found in the X-ray maps of cross sections of small GSR particles. On their surfaces, however, smaller knobs (Fig. 2c and d), spikes (Fig. 3), and bulges are seen [*3,4*]. These appear as dense surface spots in the X-ray maps of those elements that have not been shown in this report. This suggests that vapors of those elements and perhaps also lead droplets could be surface-captured in the semisolid state of GSR as they cool down from the high explosion temperature. The larger irregular spheroids (Fig. 6) and hollow-shaped GSR (Fig. 5) (diameter, $\gg 15$ μm) fall into Category II of element distribution. "Peeled oranges" fall into Category III of element distribution.

Discussion

The three categories of element distribution (Figs. 10 to 12) characterize three principal modes or stages of GSR formation. Figure 13 contains this interpretation. The top panel in Fig. 13 represents an unfired cartridge, the components of which from left to right are the firing pin, the primer, the gunpowder, and the bullet. The bottom panel shows the expected variation in temperature (°C) or pressure (psi) with time of explosion (firing). This curve is not an experimental one. It has been drawn as much as possible following curves and information from texts [*11,12*] pertaining to ignitions of primers and nitrocellulose. As the firing pin strikes the primer housing, the heat of combustion melts the primer. Within a fraction of a millisecond the primer temperature exceeds the vaporization points of lead (1620°C), antimony (1380°C), and barium (1140°C). Because of supersaturation, the primer vapors condense back onto the liquified primer surface as droplets. This nucleation under high pressure is similar to homogeneous nucleation in free space [*19,20*], except that the rate of nucleation may be influenced by a nondiffusion process [*23*]. This establishes a dynamic equilibrium in temperature (1500 to 2000°C) and pressure (9653 kPa [1400 psi]).

We have evidence suggesting that GSR particles are formed prior to the explosion of the gunpowder. Large flakes composed of only lead, antimony, and barium represent melted primer surfaces with condensed droplets (GSR) settled on them. Also, the cross sections of residue particles obtained from several firings of primer cups that had been previously removed from bullets and nitrocellulose show a great deal of homogeneity of lead, antimony, and barium.

The fluid motion in primer droplets resulting from thermal agitation and Brownian motion will possibly maintain the homogeneity of elements in these minute droplets. Thus, a majority of small residues of Category I would form at the dynamic equilibrium of the primer explosion. Some of these droplets, depending on their proximity to others, will grow rapidly by coalescence (fusion), becoming bigger and bigger. As the detonation front comprising these droplets strikes the gunpowder, they are exposed to steep rises in temperature and pressure. The small droplets experience less heat damage but suffer from greater instability in shape, owing to their higher average velocity. Note that the supplied momentum or the kinetic energy is about the same for all the droplets. The smaller droplets will travel through

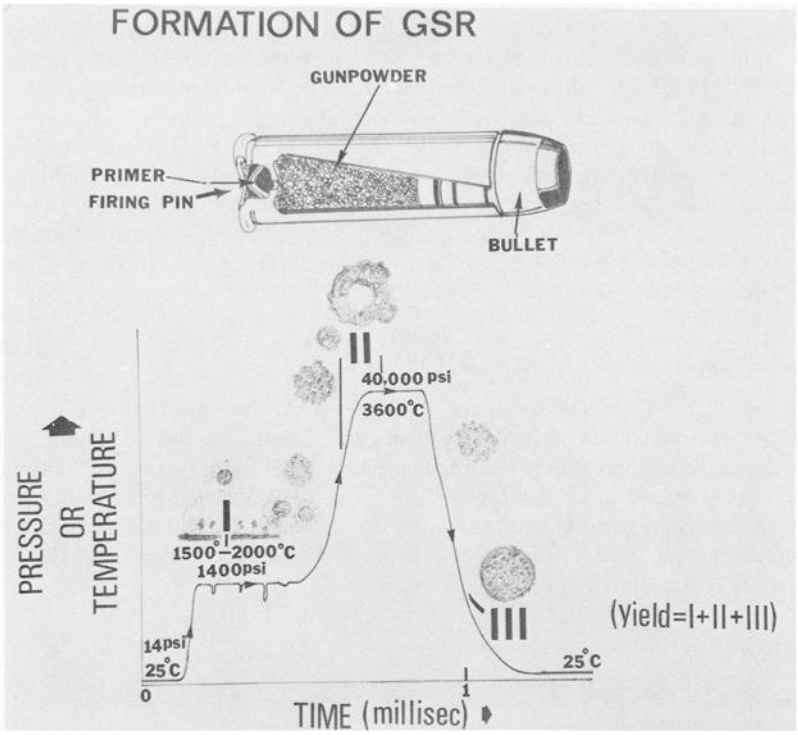

FIG. 13—*The formation of GSR via three stages (I, II, and III) of primer explosions (1 psi = 6.89 kPa).*

the high pressure and temperature zone of the propellant much faster than their larger counterparts. The larger droplets, because of their heaviness, pass through various metastable states that are due to boiling, fragmenting, or etching until their stable shape (droplet sphere, Fig. 2a) is regained.

With the onset of cooling many of these GSR particles freeze in their existing forms. The smaller ones are of Type I (regular, nodular, and irregular spheroids, Figs. 2 and 3), and the larger ones are of Type II (hollow-shaped and atypical irregular GSR, Figs. 5 and 6). While solidifying, some preformed nuclei of antimony and barium may also capture lead vapor of burnt residues and of the etched bullet. These are Type III ("peeled oranges," Fig. 4). Owing to the sharpness in cooling and because the solidification points of antimony (630.5°C) and barium (725°C) are very close, very few cores contain barium only. Rather, they contain both elements. The solidification point of lead is the lowest (327°C), and therefore lead occurs as a layer around the core in "peeled oranges." We have not seen particles with only antimony or lead as the core element.

All three elements, lead, antimony, and barium, are unified in most small GSR because their bulk phase was formed as droplets in the first equilibrium (I) of primer explosion. This hypothesis does not exclude the formation of other GSR that may capture nonspecific and bullet-derived elements on their surfaces. Obviously, these elements contribute to inhomogeneity of the GSR surfaces,which many authors have reported [*1–6*].

Conclusion

The combined study of surface morphology and cross sections of GSR by X-ray mapping of elements, mainly lead, antimony, and barium, suggests that these elements condense

from primer vapors by a principal mode. The elements condense concurrently and uniformly to form GSR droplets with a diameter up to at least 10 μm. The regular, nodular, and irregular spheroids are in this category and account for most (about 90%) of the hand-sampled GSR [*3,5,8,24*]. Although these GSR may display surface inhomogeneity owing to captured bullet elements and nonspecific elements, the homogeneity of lead, antimony, and barium in their interior can be an important criteria for their identification and for discrimination against environmental and occupational particulates [*7,8*]. The larger GSR, such as the "peeled oranges" and the hollow-shaped GSR, provide important clues to the present hypothesis of GSR formation. Unfortunately, these larger GSR fall off the firing hand much faster and are deemed to lose their significance in the detection of firearm crimes, except perhaps suicides (Fig. 4a and b).

Acknowledgments

I wish to thank Technical Sergeants Arthur Spencer, Dominic Denio, and Charles E. Boone for their cooperation in the test firing of guns. Thanks are also due to Robert Miazga for his assistance in photography and to Donna Lee Heald for her technical assistance. Appreciation is expressed to Captain Stark Ferriss and Lieutenant Robert W. Horn for their continued interest in gunshot residue studies and for many helpful discussions during the development of the present work. I am also grateful to Charles Turner, SAAMI, for providing many technical details of primer explosion.

References

[*1*] Nesbitt, R. S., Wessel, J. E., and Jones, P. F., "Detection of Gunshot Residue by Use of the Scanning Electron Microscope," *Journal of Forensic Sciences,* Vol. 21, No. 3, July 1976, pp. 595–610.

[*2*] Andrasko, J. and Maehly, A. C., "Detection of Gunshot Residues on Hands by Scanning Electron Microscopy," *Journal of Forensic Sciences,* Vol. 22, No. 2, April 1977, pp. 279-287.

[*3*] Matricardi, V. R. and Kilty, J. W., "Detection of Gunshot Residue Particles from the Hands of a Shooter," *Journal of Forensic Sciences,* Vol. 22, No. 4, Oct. 1977, pp. 725–738.

[*4*] Tassa, M. and Zeldes, N., "Characterization of Gunshot Residue Particles by Localizations of Their Chemical Contituents," *Scanning Electron Microscopy,* Part II, 1979, SEM, Inc., AMF O'Hare, II, pp. 175–178.

[*5*] Wolten, G. M., Nesbitt, R. S., Calloway, A. R., Loper, G. L., and Jones, P. F., "Particle Analysis for the Detection of Gunshot Residue. I: Scanning Electron Microscopy/Energy Dispersive X-ray Characterization of Hand Deposits from Firing," *Journal of Forensic Sciences,* Vol. 24, No. 2, April 1979, pp. 409-422.

[*6*] Basu, S. and Ferriss, S., "A Refined Collection Technique for Rapid Search of Gunshot Residue Particles in the SEM," *Scanning Electron Microscopy,* Part I, 1980, SEM, Inc., AMF O'Hare, II, pp. 375-384; 392.

[*7*] Buckle, E. R., "Nature and Origin of Particles in Condensation Fume: A Review," *Journal of Microscopy,* Vol. 114, No. 2, Nov. 1978, pp. 205-214.

[*8*] Wolten, G. M., Nesbitt, R. S., Calloway, A. R., and Loper, G. L., "Particle Analysis for the Detection of Gunshot Residue. II: Occupational and Environmental Particles," *Journal of Forensic Sciences,* Vol. 24, No. 2, April 1979, pp. 423-430.

[*9*] Buckle, E. R. and Pointon, K. C., "Condensation of Zinc Aerosols," *Journal of Materials Science,* Vol. 12, No. 1, Jan. 1977, pp. 75-89.

[*10*] Buckle, E. R. and Tsakiropoulos, P., "Crystallography of Metallic Aerosol Precipitates: Dendritic Origin of Hexogonal Prisms in Cd and Zn," *Journal of Materials Science,* Vol. 14, No. 6, June 1979, pp. 1421-1424.

[*11*] Cook, M. A., *The Science of High Explosives,* American Chemical Society Monograph Series, Reinhold Publishing Corp., New York, 3rd printing, 1963, Chapters 6-8, pp. 123-205.

[*12*] Wolten, G. M. and Nesbitt, R. S., "On the Mechanism of Gunshot Residue Particle Formation," *Journal of Forensic Sciences,* Vol. 25, No. 3, July 1980, pp. 533-545.

[*13*] Robinson, V. N. E., "Imaging with Backscattered Electrons in a Scanning Electron Microscope," *Scanning,* Vol. 3, No. 1, 1980, pp. 15-26.

[*14*] Reimer, L. and Tollkamp, C., "Measuring the Backscattering Coefficient and Secondary Electron Yield Inside a Scanning Electron Microscope," *Scanning,* Vol. 3, No. 1, 1980, pp. 35-39.

[15] Zeldes, N. and Tassa, M., "Conversion of Existing SEM Components to Form an Efficient Backscattered Electron Detector, and Its Forensic Applications," *Scanning Electron Microscopy,* Part II, 1979, SEM, Inc., AMF O'Hare, II, pp. 155-158; 124.

[16] Russ, J. C., "X-Ray Mapping on Irregular Surfaces," *The EDAX Editor,* Vol. 9, No. 2, 1979, pp. 10-11.

[17] Reimer, L., "Electron-Specimen Interactions," *Scanning Electron Microscopy,* Part II, 1979, SEM, Inc., AMF O'Hare, II, pp. 111-124.

[18] Russ, J. C., "New Methods to Obtain and Present SEM X-Ray Line Scans," *The EDAX Editor,* Vol. 9, No. 2, 1979, pp. 3-9.

[19] Wegener, P. P. and Parlange, J-Y., "Condensation by Homogeneous Nucleation in the Vapor Phase," *Naturwissenschaften,* Vol. 57, No. 11, 1970, pp. 525-533.

[20] Derjaguin, B. V., "General Theory of Nucleation I. Theory of Homogeneous Condensation upon Moderate Supersaturation," *Journal of Colloid and Interface Science,* Vol. 38, No. 2, Feb. 1972, pp. 517-522.

[21] Newbury, D. E., "Microanalysis in the Scanning Electron Microscope: Progress and Prospects," *Scanning Electron Microscopy,* Part II, 1979, SEM, Inc., AMF O'Hare, II, pp. 1-20.

[22] Marshall, A., *Explosives: Their Theory, Manufacture, Properties and Tests,* Vol. VII, Chapter 29, 1932, J. A. Churchill, London, pp. 133-142.

[23] Bradley, R. S., "The Rate of Nucleation at High Pressures," *Journal of Colloid Science,* Vol. 15, No. 6, Dec. 1960, pp. 525-530.

[24] Wallace, J. S. and Keeley, R. H., "A Method for Preparing Firearms Residue Samples for Scanning Electron Microscopy," *Scanning Electron Microscopy,* Part II, 1979, SEM, Inc., AMF O'Hare, II, pp. 179-184.

Address requests for reprints or additional information to
Samarendra Basu, Ph.D.
New York State Police Crime Laboratory
NYS Police Headquarters
State Campus, Bldg. 22
Albany, NY 12226